Available online at www.sciencedirect.com
ScienceDirect
Journal of Organometallic Chemistry 691 (2006) 4434–4445
Journal of Organometallic Chemistry
www.elsevier.com/locate/jorganchem

Formation of pyridine from acetylenes and nitriles catalyzed by RuCpCl, CoCp, and RhCp derivatives – A computational mechanistic study

Georg Dazinger [a], Marta Torres-Rodrigues [a], Karl Kirchner [a,*], Maria José Calhorda [b], Paulo J. Costa [b]

[a] *Institute of Applied Synthetic Chemistry, Vienna University of Technology, Getreidemarkt 9, A-1060 Vienna, Austria*
[b] *Departamento de Química e Bioquímica, Faculdade de Ciências, Universidade de Lisboa, 1749-016 Lisboa, Portugal*

Received 31 December 2005; received in revised form 17 February 2006; accepted 1 March 2006
Available online 8 March 2006

Abstract

The mechanism of the catalytic formation of pyridines from the coupling of two alkynes and the nitriles N≡CR (R = H, Me, Cl, COOMe) with the fragments CpRuCl, CpCo, and CpRh has been investigated by means of DFT/B3LYP calculations. According to the proposed mechanism, the key reaction step is the oxidative coupling of two alkyne ligands to give metallacyclopentatriene (Ru, Rh) and metallacyclopentadiene (Co) intermediates. In the case of ruthenium, this process is thermodynamically clearly favored over the oxidative coupling between one alkyne and one nitrile ligand to afford an azametallacycle. This alternative pathway however cannot be dismissed in the case of Co and Rh. The rate determining step of the overall catalytic cycle is the addition of a nitrile molecule to the metallacyclopentatriene and metallacyclopentadiene intermediates, respectively, which has to take place in a side-on fashion. Competitive alkyne addition leads to benzene formation. Thus, also the chemoselectivity of this reaction is determined at this stage of the catalytic cycle. In the case of the RuCpCl fragment, the addition of nitriles R–C≡N and acetylenes RC≡CH has been studied in more detail. For R = H, Cl, and COOMe the side-on addition of nitriles is kinetically more favored than alkyne addition and, in accordance with experimental results, pyridine formation takes place. In the case of R = Me nitrile addition could not be achieved and the addition of alkynes to give benzene derivatives seems to be kinetically more favored. Once the nitrile is coordinated facile C–C bond coupling takes place to afford an unusual five- and four-membered bicyclic ring system. This intermediate eventually rearranges to a very unsymmetrical azametallaheptatriene complex which in turn provides CpRuCl(κ^1-pyridine) via a reductive elimination step. Completion of the catalytic cycle is achieved by an exergonic displacement of the respective pyridine product by two acetylene molecules regenerating the bisacetylene complex.

Keywords: Ruthenium; Cobalt; Rhodium; Alkynes; Nitriles; Cycloaddition; Pyridine formation; DFT calculations

1. Introduction

The elucidation of the mechanistic aspects of homogeneous catalysis has been an ambitious scientific goal from the beginning of the awareness of organometallic catalysis. However, kinetic studies often fail to give a complete mechanistic picture of catalytic reactions, since the rates of the successive steps and stabilities of the diverse reaction intermediates are too little divergent to be separately observed and characterized especially in the case of catalytic processes. Due to the enormous progress in computational chemistry in the last several years, theoretical methods are playing an increasingly important role in identifying possible elementary reactions [1]. Ultimately, one would

* Corresponding author. Tel.: +43 1 58801 15341; fax: +43 1 58801 15499.
E-mail address: kkirch@mail.zserv.tuwien.ac.at (K. Kirchner).

0022-328X/$ - see front matter © 2006 Elsevier B.V. All rights reserved.
doi:10.1016/j.jorganchem.2006.03.004

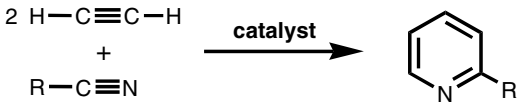

Scheme 1.

like to understand these fundamental transformations in order to be able to monitor and tune changes in reactivity toward an obvious synthetic purpose.

A reaction which falls into this category is the transition metal-mediated cyclocotrimerization of two alkynes with nitriles to afford pyridine rings (Scheme 1). Such a process has received considerable attention in recent years since it is synthetically useful, atom-economic, and environmentally benign [2]. Although a variety of stoichiometric methods have been described [3,4], catalytic systems are confined to iron [5], ruthenium [6], cobalt [7], rhodium [8], and nickel [9]. The detailed mechanism of these reactions is not yet fully established. The initial steps could be identical to those calculated previously for the cyclotrimerization of acetylenes using RuCp(COD)Cl [10,11] and $CoCp(PH_3)_2$ [12] as the model precatalyst as displayed in Scheme 2. Accordingly, the reaction would be initiated by the replacement of the labile ligands COD and PH_3, respectively, by two molecules of acetylene giving a bisacetylene complex which then transforms into a metallacyclopentadiene (for Co) or a metallacyclopentatriene (for Ru) as the result of oxidative coupling (pathway 1). These metallacycles would then insert the N≡C triple bond of a nitrile into one of the two metal–carbon bonds leading to several possible intermediates. Alternatively, the catalytic reaction might also proceed via the azametallacycles formed by coupling of one alkyne and one nitrile molecule (pathway 2). Subsequent insertion of a second alkyne molecule into either the metal–N or metal–C bond could lead to the formation of several intermediates, some of them coincident with those formed in pathway 1. A theoretical investigation of the cyclocotrimerization of nitriles and acetylenes has been reported recently by Yamamoto and co-workers [6] where it has been suggested that pathway 1 is favored.

In this paper we report the results of our theoretical examination of plausible mechanisms for the cyclocotrimerization of alkynes with the model nitriles N≡C–R (R = H, Me, Cl, COOMe) to afford pyridine rings, based on DFT/B3LYP calculations. Continuing our recent theoretical studies [10,13], we have chosen as model pre-catalysts CpRu(COD)Cl as well as CoCp(COD) (a classic alkyne trimerization catalyst), and RhCp(COD), since we are also interested in understanding reactivity changes within homologous series. It has to be mentioned that experimentally ruthenium catalysts work only if electron-deficient nitriles are utilized [6], while electron-rich nitriles do not react and instead alkyne cyclotrimerization to give benzene derivatives becomes the predominant process. With cobalt catalysts, on the other hand, this pattern is reversed and electron-rich nitriles appear to be more effective [7].

2. Results and discussion

2.1. The RuCpCl system

Based on DFT/B3LYP [14] calculations using GAUSSIAN03 [15], three pathways are in principle conceivable for the conversion of two alkynes and one nitrile into free pyridine, catalyzed by RuCp(COD)Cl. Pathway 1 proceeds via a ruthenacyclopentatriene intermediate (B), which also plays a major role in alkyne cyclotrimerization, and will thus be studied first. The two alternative pathways 2 and 3 involve the intermediacy of an experimentally, as yet, elusive azaruthenametallacyclopentadiene B^N, but differ in the coupling of the second alkyne. The potential free energy surface (in kcal/mol) for the first step in the reaction, namely the formation of the metallacycle intermediates, is given in Scheme 3.

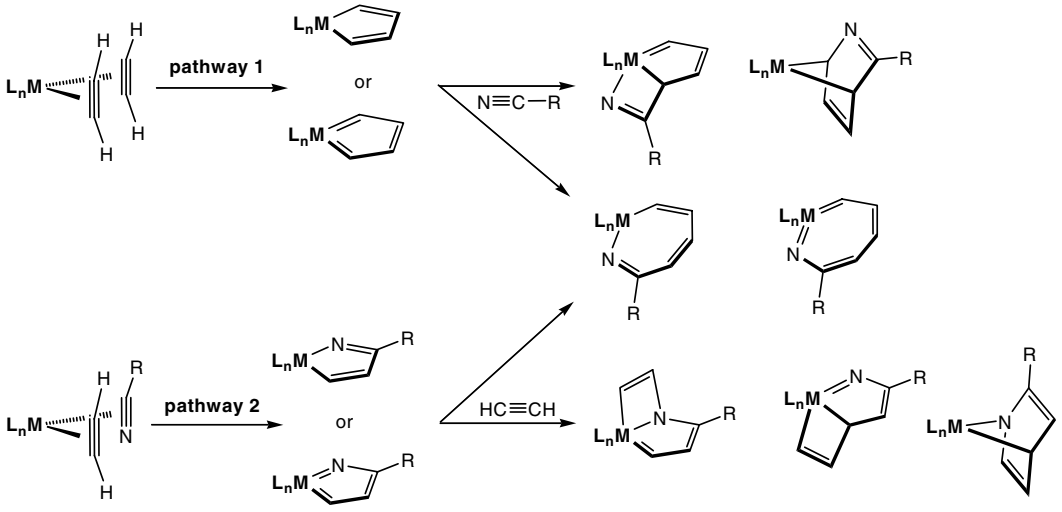

Scheme 2.

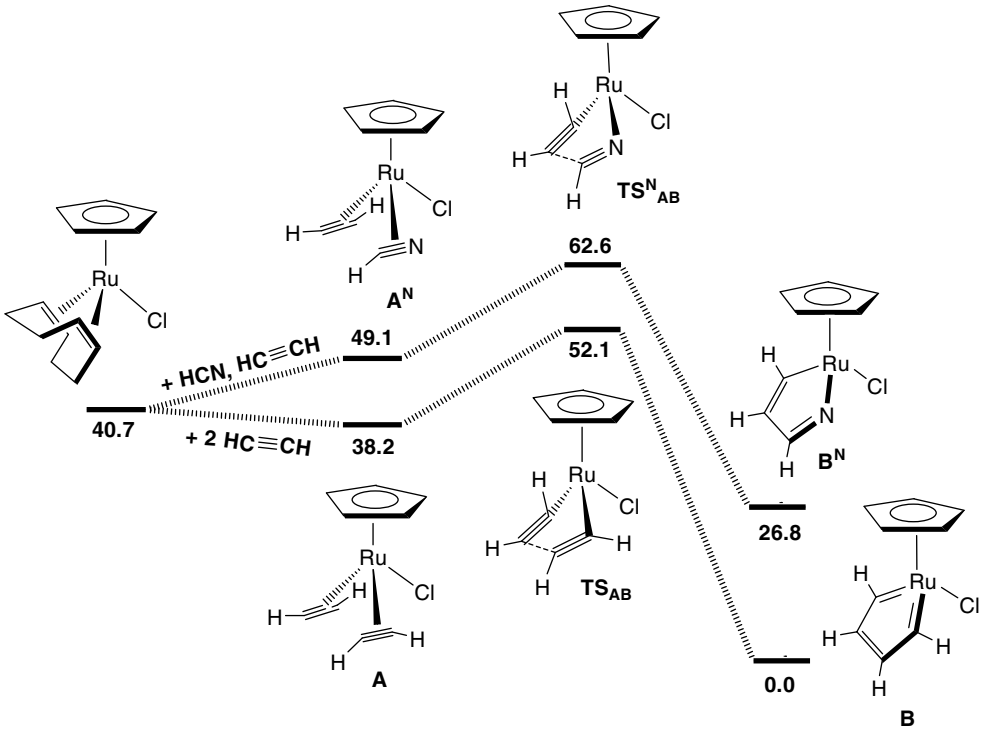

Scheme 3. Free energy profile (in kcal mol^{-1}) for the conversion of RuCp(COD)Cl via intermediates A and A^N into the respective metallacycles B and B^N.

For pathway 1, the initial step is the replacement of labile COD by two molecules of acetylene to afford via the bisacetylene complex A the metallacyclopentatriene B. Both steps are exergonic releasing 2.5 and 38.2 kcal/mol, respectively. For pathways 2 and 3, on the other hand, the substitution of COD by one molecule of acetylene and one molecule of nitrile to give the nitrile-acetylene complex A^N is endergonic (8.4 kcal/mol), while the subsequent formation of the azametallacycle B^N is again strongly exergonic by 22.3 kcal/mol. Interestingly, regardless of whether two acetylenes or one acetylene and one nitrile are oxidatively coupled, the free activation energies for these two alternative processes are very similar (13.9 and 13.5 kcal/mol, respectively). The formation of ruthenacyclopentatriene B is thermodynamically clearly favored, however. The potential free energy surfaces (in kcal/mol) for the three alternative pathways 1, 2, and 3 are given in Schemes 4, 6 and 7. The conversion of the ruthenacyclopentatriene B into the η^1-pyridine complex F is addressed first using four different nitriles N≡C–R (R = H, Me, Cl, COOMe).

The addition of nitrile N≡C–R to intermediate B affords the metallacyclopentadiene C, where the nitrile is side-on coordinated (Scheme 4). The detailed structures of complexes C and transition states TS_{BC} are displayed in Fig. 1. This reaction is both kinetically and thermodynamically unfavorable. In fact, the formation of C is the rate determining step of the catalytic cycle. The free activation energy and the free energy, respectively, required for this step increases in the order H < Me < Cl < COOMe. It should be noted, however, that when R = Me all efforts to locate a stationary point for a transition state connecting B and C resulted in collapse of the structure to transition state TS_{BCe}, leading to end-on coordination of the nitrile (C_e). Indeed, the nitrile is already nearly end-on coordinated at TS_{BCe} (the Ru–N distance is 2.81 Å) (Scheme 4). The free energy barrier for the end-on coordination reaction of acetonitrile is 14.5 kcal/mol. The addition of CH_3CN is also endergonic by 8.9 kcal/mol, emphasizing the high stability of B (18e species). This is in sharp contrast to the analogous cobalt and rhodium metallacycles B, where the addition of acetylene is strongly exergonic (vide infra). It is also interesting to note that no direct equilibrium between complexes C, with the nitrile coordinated in side-on, and C_e, with the nitrile end-on bound, could be found [16].

Once complex C is formed it undergoes facile C–C bond coupling to give the azaruthenabicyclo[3.2.0]heptatriene D. This transformation is exergonic in the case of R = H, Cl, and COOMe, releasing 2.9, 18.3 and 10.7 kcal/mol, respectively, but is slightly endergonic for R = Me (2.9 kcal/mol). The transition state for this process, TS_{CD}, is very similar to the structure of C with a long C_α–$C_{nitrile}$ bond distance in the range 1.9–2.1 Å, indicating that the transition state structure occurs quite early along the reaction coordinate. Energetically, this transition state lies 0.8–3.2 kcal/mol higher than C (Scheme 4). In the case of R = Me, however, the free activation energy is higher (7.9 kcal/mol). Complex D contains an unusual five and four-membered bicyclic ring system with one Ru–C double bond (1.95 Å), one Ru–C single bond (2.19 Å), and one Ru–N single bond (2.09 Å). As the reaction proceeds, and the new C–C bond starts to form, the Ru–C_α distance of the bond directly

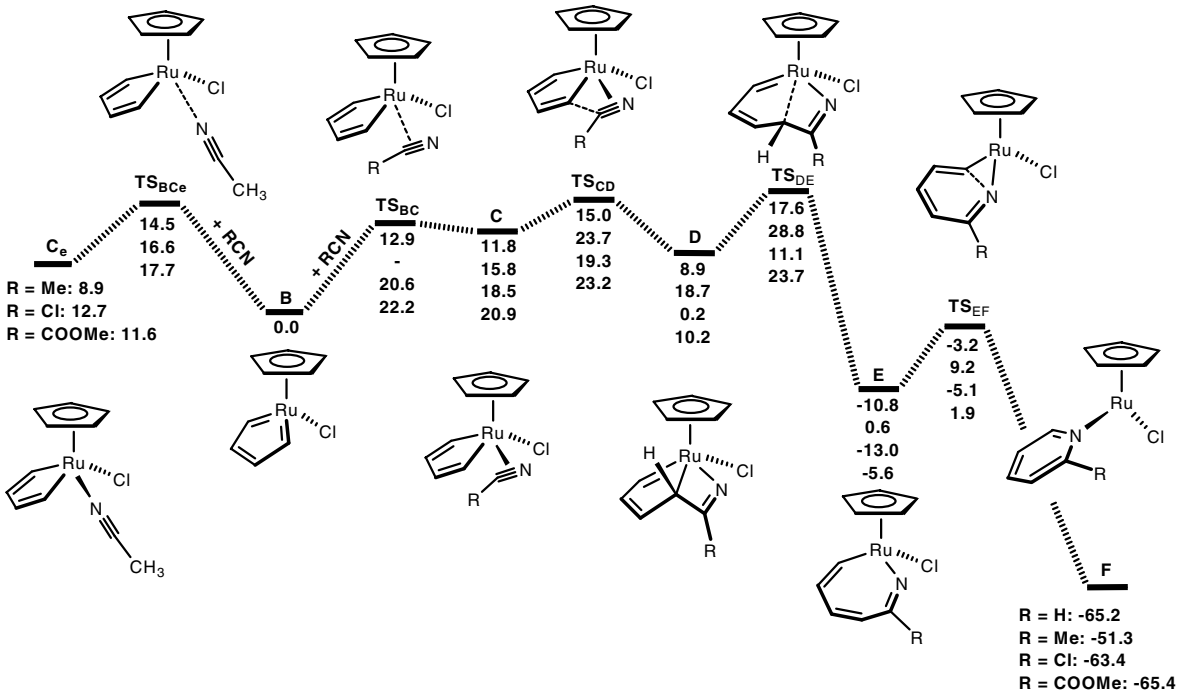

Scheme 4. Free energy profile (in kcal mol^{-1}) for the conversion of the ruthenacycle B into the η^1-pyridine complex F with various nitriles N≡C–R (R = H, Me, Cl, COOMe).

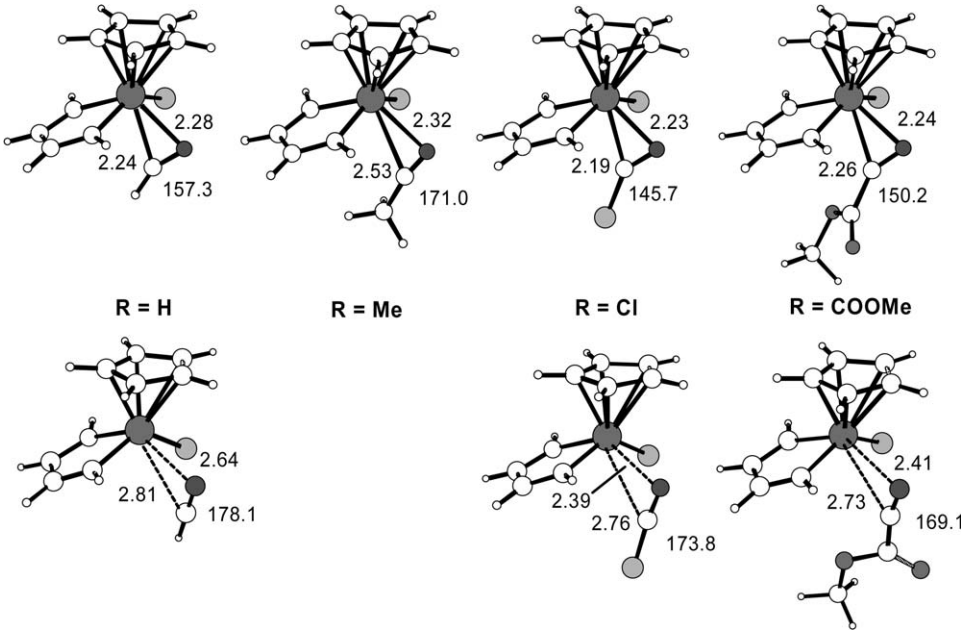

Fig. 1. Optimized geometries (distances in Å, angles in °) of intermediates C (top) and TS_{BC} (bottom) of the CpRuCl system with N≡C–R.

involved in the C–C coupling process increases slightly from about 2.0 Å in C to 2.1 Å in TS_{CD} and 2.2 Å in D. The detailed structure of D is given in Fig. 2. It is very important to mention, however, that the transformation of C to D via TS_{CD} becomes difficult if C bears α-substituents, since after C_α–$C_{nitrile}$ coupling the substituent (in the model system a hydrogen atom, complex D) is pointing towards the Cp ligand giving rise to repulsive interligand interactions (Fig. 2). In fact, as has been shown experimentally [6], the catalytic cyclocotrimerizations of alkynes and nitriles by RuCp*(COD)Cl takes place only if the alkyne to be coupled is a 1,6-diene bearing at least one terminal hydrogen atom [6].

Complex D rearranges easily via transition state TS_{DE} to afford the azametallacycle E. In the course of this process, the internal Ru–C single bond is cleaved. This

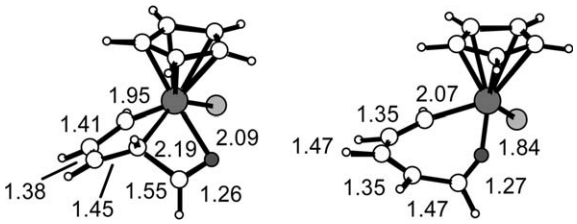

Fig. 2. Optimized geometries (distances in Å) of the intermediates D and E of the CpRuCl system with parent HCN.

reaction requires a free activation energy of 8–14 kcal/mol, depending on the nitrile, and is, with the exception of R = Me, thermodynamically very favorable. Complex E features a non-planar asymmetric seven-membered metallacyclic ring (Fig. 2) with Ru–C and Ru–N single bonds. The C–C bond distances within the metallacycle show a long–short–long pattern.

The final intermediate in the catalytic cycle of Scheme 4 is complex F exhibiting a κ^1-coordinated pyridine ligand. The loss of the resonance stabilization energy upon pyridine formation combines with the construction of a new carbon–carbon σ-bond to release 42–68 kcal/mol, depending on R. The completion of the catalytic cycle in Scheme 4 requires the displacement of the pyridine ligand in F by two alkynes. Thermodynamically, the barrier to overcome this process is the Ru–nitrogen binding energy which appears to be small (weak Ru–N bond). The energetic consequences of the displacement of pyridine by two alkynes to give the respective pyridine and A is exergonic by 3.3, 5.5, 10.8, and 0.4 kcal/mol for R = H, Me, Cl, and COOMe, respectively, showing that pyridine displacement is thermodynamically indeed accessible. The full catalytic cycle is shown in Scheme 5.

Although the formation of the azaruthenacycle B^N is thermodynamically less favorable than that of B, we also took a closer look at pathways 2 and 3, which involve this intermediate (Schemes 6, 7). Due to the asymmetric nature of B^N, alkyne addition may occur either at the N- or C-site. The free energy barriers for these processes are 10.7 kcal/mol (N-site) and 18.3 kcal/mol (C-site) and afford the metallacyclopentadiene complexes C^N and G^N, respectively. The formation of these complexes is endergonic by 5.9 and 10.4 kcal/mol. Accordingly, the addition of an incoming alkyne is both kinetically and thermodynamically favored at the N site.

In the onward reaction of C^N, a new C–N bond is established and the unusual azaruthenabicyclo[3.2.0]heptatriene D^N is formed. This conversion is strongly exergonic, releasing 35.4 kcal/mol. The optimized geometry of D^N, with selected bond distances, is given in Fig. 3. This species contains an almost planar bicylic ring system with two Ru–C carbon single bonds (2.06 and 2.10 Å) and one Ru–N single bond (2.06 Å). D^N appears to be an extremely stable compound, making both the subsequent reductive elimination to give the η^2-pyridine complex E^N via TS^N_{DE}, as well as the back reaction to yield C^N, kinetically very unfavorable (48.5 and 42.3 kcal/mol, respectively). Thus, this pathway may be dismissed as non competitive and D^N can be regarded as a dead-end product, which actually might be isolable or, at least, detectable spectroscopically. To the best of our knowledge, however, this has not happened.

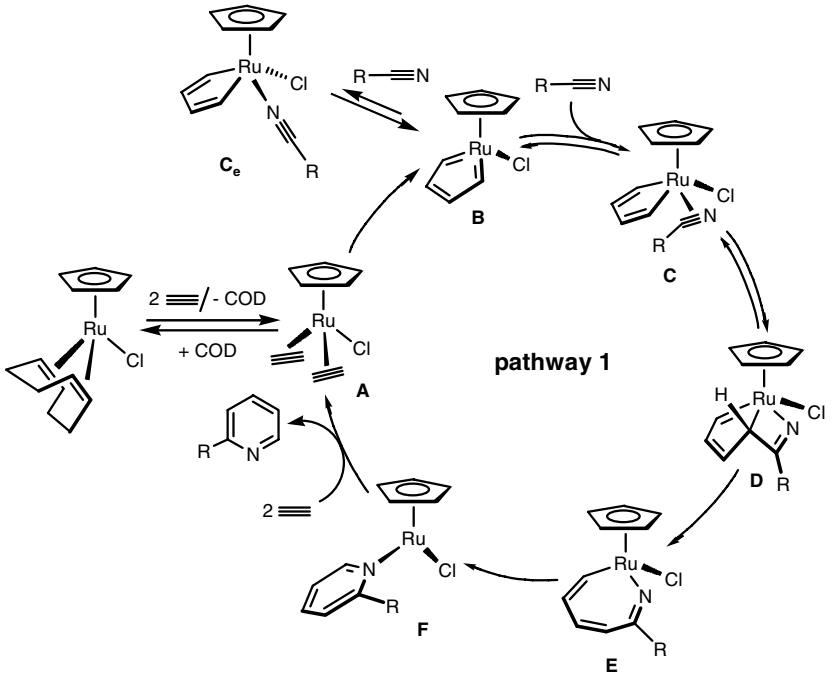

Scheme 5.

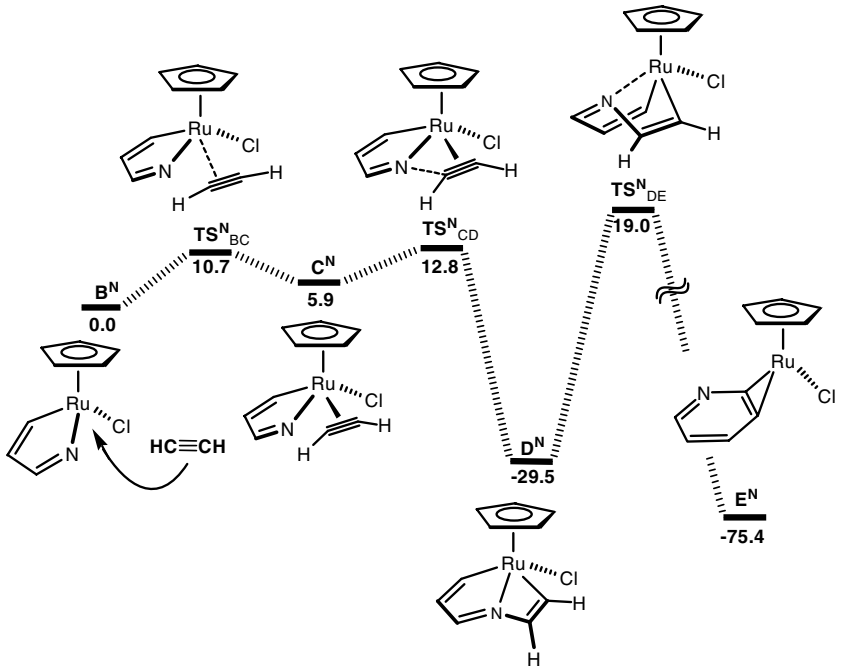

Scheme 6. Free energy profile (in kcal mol^{-1}) for the conversion of the aza-metallacycle B^N into the η^2-pyridine complex E^N via alkyne addition at the N-site.

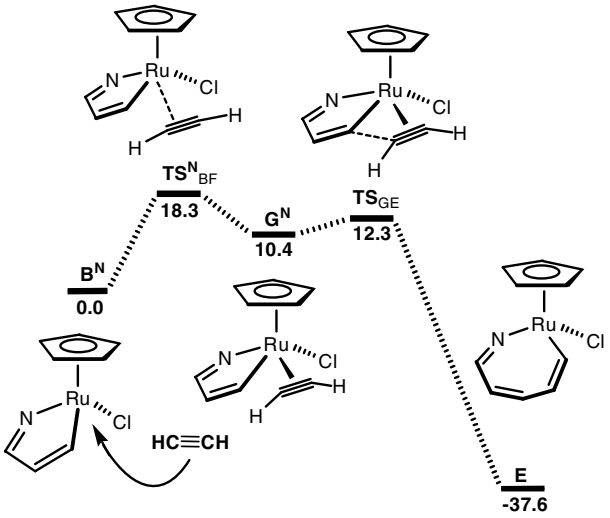

Scheme 7. Free energy profile (in kcal mol^{-1}) for the conversion of the aza-metallacycle B^N into the metallacyclic complex E via initial alkyne attack at the C-site.

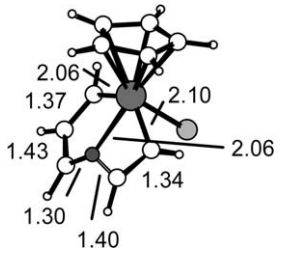

Fig. 3. Optimized geometry (distances in Å) of intermediate D^N of the CpRuCl system.

Pathway 3, on the other hand, leads to the same intermediate E as pathway 1, but involves higher activation energies in the initial steps (Scheme 3). In sum, the above results may suggest that the ruthenium catalyzed formation of pyridine is unlikely to take place via pathways 2 and 3.

Pathway 1 shares the first step of the reaction with the mechanism for the formation of benzene by the RuCpCl catalyst (formation of the active species, the metallacycle B). Since there is excess of alkyne present, a competition between acetylene and nitrile as ligands to the metallacycle B takes place. The energetics for these reactions is given in Scheme 8. While benzene formation is thermodynamically preferred, the activation barriers for the binding of acetylenes and nitriles are comparable and strongly dependent on the substituents. With R = H and COOMe, the addition of nitriles to afford pyridines is kinetically more facile than the addition of acetylenes, while with R = Me, in accordance with experimental results, this pattern is reversed and the formation of benzene is favored.

Another important aspect of these reactions concerns the nitrile coordination mode. In all the examples studied, end-on coordination leads to a more stable species than side-on coordination (Scheme 4), but the coupling reaction with the metallacycle carbon only takes place for the side-on coordination. Also, it has not been possible to find a transition state connecting the end-on complex C$_e$ to the side-on one C. This results contradicts the proposal for the mechanism as studied by Yamamoto and co-workers [11], where such a transformation was assumed, but, on the other hand, these authors did not study this step in detail (no transition state is given). In order to understand this competition between end-on and side-on coordination,

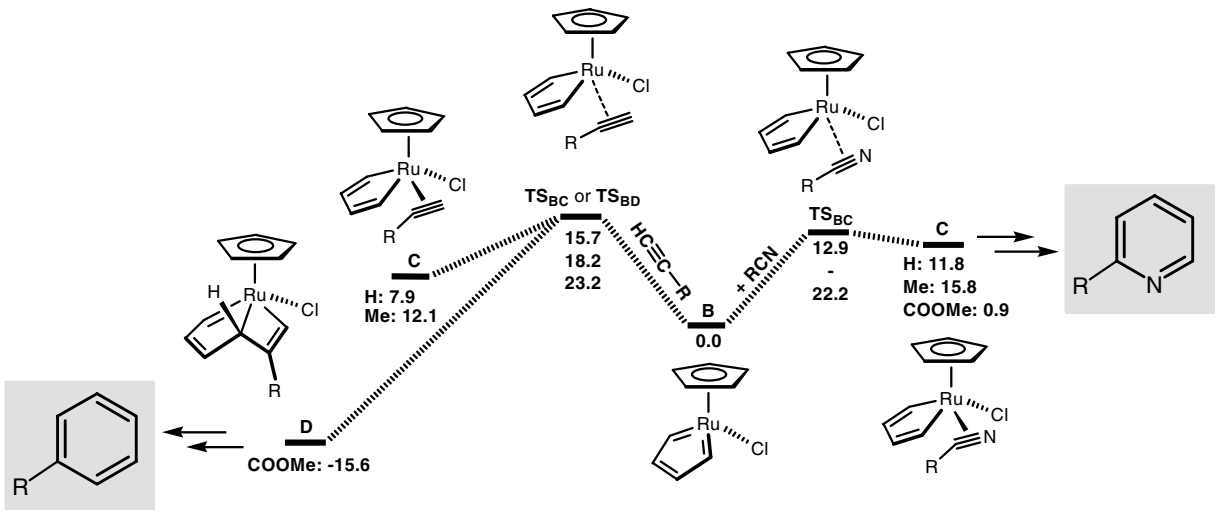

Scheme 8. Free energy profile (in kcal mol^{-1}) for the competitive addition of N≡C–R and HC≡C–R (R = H, Me, COOMe) to the ruthenacycle B.

we should start by revisiting the bonding of a nitrile ligand to a metal center.

A Molekel [17] three-dimensional representation of the relevant orbitals of N≡CMe is shown in Fig. 4 (left side) [18].

When the nitrile bends, the degenerate π and π* sets of orbitals lose their degeneracy. The in-plane orbitals mix with σ and become hybridized in such a way, that overlap with the metal orbitals increases (right side of Fig. 4) [19]. The energy of π_i^* becomes significantly lower, so the ligand is expected to become a better π acceptor. The behavior of π_i is not so clear, owing to mixing of the Cl p orbitals. A schematic molecular orbital (Fig. 5) represents the interaction between the RuCpCl(C_4H_4) fragment and end-on (left) and side-on (right) N≡C–Cl.

When end-on coordinated, nitriles bind essentially as σ-donor or weak π-donor. The end-on bound N≡C–Cl acts mainly as a σ donor (Fig. 5, left). Other nitriles, such as N≡C–Me, can also behave as weak π donors. This results from the electronegativity difference between C and N,

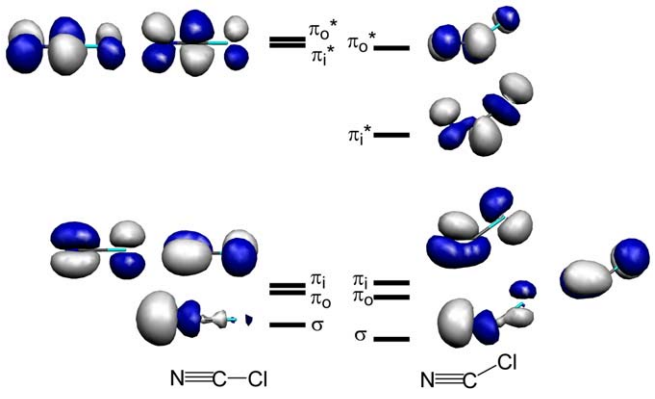

Fig. 4. Frontier orbitals (Molekel) [17] of linear (left) and bent (right) N≡C–Cl.

which leads to a higher localization in the nitrogen atom in the π than in the π* orbital (Fig. 4), and thus to a larger M–N overlap with π than with π*. On the other hand, in the side-on nitrile, the σ-donor component involves the π_l level, with mixing of a lower level. There is also a back donation interaction between the occupied orbital of the Ru fragment and the π_i^*. In this way, the nitrile acts as a π-ligand, donating electrons from π_l and receiving in π_i^*. Globally, it becomes a π-acceptor.

The preference for end-on vs side-on binding is directly related to the back donation capabilities of the metal center. Let us now analyze the binding of the four nitriles studied to the RuCpCl fragment. In order to do that, we performed an energy decomposition analysis, using the ADF program [20] and the optimized geometries described above. The results are collected in Table 1. The interaction energy, ΔE_{int}, between fragments can be divided into three main components

$$\Delta E_{int} = \Delta E_{elec} + \Delta E_{Pauli} + \Delta E_{orb},$$

where ΔE_{elec} gives the electrostatic interaction energy between the fragments, ΔE_{Pauli} refers to the repulsive interactions between the fragments, and ΔE_{orb} is the stabilizing orbital interaction term. The bond dissociation energy can be calculated from this interaction energy ΔE_{int} by adding ΔE_{prep}, the energy needed to promote the fragments from their equilibrium geometry to the geometry in the complexes [21]. The first interesting conclusion is that the orbital interaction ΔE_{orb} is larger for all nitriles when side-on bonded, except for N≡C–Me. This results directly from the shape of the frontier orbitals of the RuCpCl(C_4H_4) fragment with the geometry displayed in complexes C, which are shown in Fig. 5 (center; LUMO on top and HOMO on bottom). The LUMO has the symmetry to receive electrons from the σ or the π nitrile orbital, depending on the coordination mode, while the HOMO is apt for backdonation. On the other hand, the repulsive

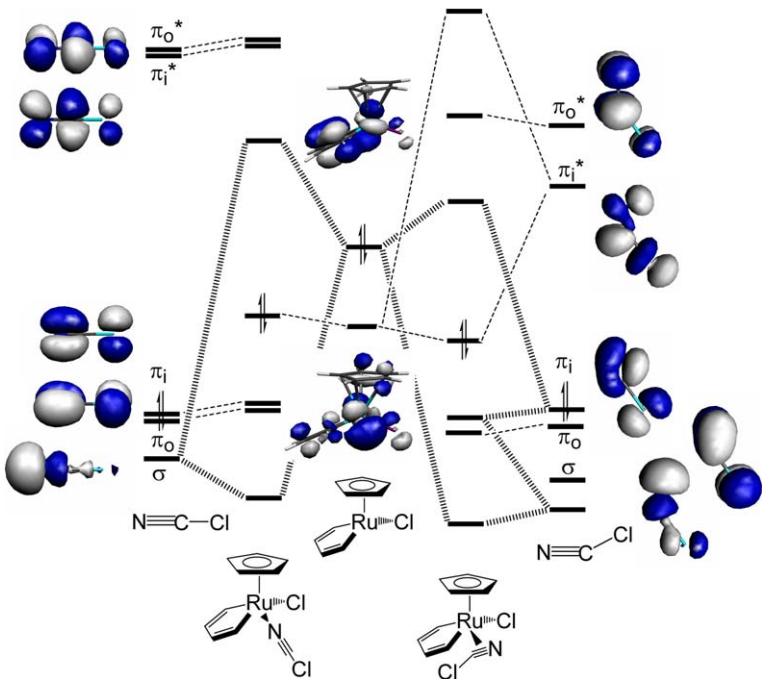

Fig. 5. Schematic interaction diagram between the $RuCpCl(C_4H_4)$ fragment and end-on (left) and side-on (right) N≡C–Cl.

Table 1
Energy decomposition for the interaction between nitrile and the $RuCp(C_4H_4)Cl$ fragment in complexes C and C_e (energies in kcal/mol)

	N≡CMe		N≡CCl		N≡CCOOMe		N≡CH	
	End-on	Side-on	End-on	Side-on	End-on	Side-on	End-on	Side-on
BE′	−26.13	−19.28	−23.94	−35.15	−27.81	−27.32	−25.33	−25.95
ΔE_{Pauli}	110.35	79.47	107.44	148.12	120.64	127.69	113.53	123.91
ΔE_{elec}	−79.89	−55.80	−75.03	−89.37	−82.87	−77.08	−79.16	−76.33
ΔE_{st}	30.46	23.68	32.41	58.74	37.77	50.6	34.37	47.59
ΔE_{orb}	−56.59	−42.96	−56.35	−93.89	−65.58	−77.93	−59.70	−73.54
$\Delta E_{prep\ (Ru)}$	16.17	15.14	16.51	17.51	16.88	17.22	16.73	17.19
$\Delta E_{prep(nit)}$	0.03	1.09	0.00	11.41	0.04	5.56	0.00	4.18
BE	−9.37	−2.98	−7.37	−6.21	−10.89	−4.47	−8.55	−4.59
d(C–N)	1.156	1.176	1.158	1.205	1.158	1.194	1.154	1.189
∠C–N–X	178.1	171.0	179.1	145.7	176.3	150.2	178.5	157.3
d(C–N)[a]	1.160		1.160		1.160		1.159	
∠C–N–X[a]	179.7		180.0		176.8		180.0	

[a] Optimized free nitriles.

terms (ΔE_{st}) corresponding to the sum of the Pauli repulsion and the electrostatic interaction are positive (repulsive) and larger for side-on nitriles. This reflects larger steric repulsion in this case. Also, for side-on nitriles, the preparation energies are large, as the molecule has to bend. Notice the large values for the highly bent N≡C–Cl and N≡CCOOMe. These terms will cancel the ΔE_{orb} term, so that side-on bonding is energetically less favorable. The closest binding energies are observed for N≡C–Cl, where the electronegativity of chlorine makes it a very good π-acceptor ligand (large bending angle). At the other extreme lies N≡CMe. Methyl is an electron donor, so side-on bonding is unfavored. Indeed, the ligand barely bends, and the binding energy is the smallest (−2.98 kcal/mol), with long Ru–N and specially Ru–C bonds. The $RuCpCl(C_4H_4)$ fragment is very similar for all complexes, despite the coordination mode of the nitrile and require a large preparation energy to distort enough to allow coordination of the nitrile. The preparation energy ranges from ca 15–17 kcal/mol.

The activation of the nitrile provided by side-on coordination activates the C–N bond toward further reaction. The C–N bonds are longer in all cases, accompanying bending, and therefore weaker. Despite the lower energy of the end-on complexes, the difference is small and the C–N bond is not so reactive.

2.2. The CoCp and RhCp systems

In the main aspects, the results of our computational studies on the CpCo and CpRh systems are similar to those of the CpRuCl fragment as pathway 1 is concerned. The initial steps again are the replacement of labile COD by two molecules of acetylene to afford the bisacetylene complex A which then undergoes oxidative coupling to give metallacycles B (Scheme 9 for Co). As Co and Rh behave very similarly, only the result for Co is shown (Rh is given as Supplementary material). The substitution step for the two metal fragments is in both cases essentially thermoneutral, while the coupling of the two alkynes is exergonic releasing 20.8 and 7.5 kcal/mol for Co and Rh, respectively. It should be noted that the nature of the metallacycle B varies with the metal. While in the CpCo system B behaves as a metallacyclopentadiene, it is better formulated as a metallacyclopentatriene with a bis-carbene functionality in the CpRh analog [13e].

For pathway 2, the substitution of COD by one molecule of acetylene and one molecule nitrile to give the nitrile-acetylene complex A^N is endergonic (Co, 3.0 kcal/mol; Rh, 8.7 kcal/mol). In contrast to the azaruthenacyclopentadiene B^N (see Scheme 3), in the case of Co and Rh the formation of the azametallacycle B^N is almost thermoneutral (exergonic by 3.0 kcal/mol for Co, endergonic by 2.6 kcal/mol for Rh). However, the free energy barrier for the oxidative coupling step is by and large the same in all cases, independent of the metal fragment, regardless of whether two alkynes or one alkyne and one nitrile are coupled with one another, and is in the range of 12.7–16.0 kcal/mol. The free energy profiles for the Co and Rh catalyzed pyridine formation, starting from the alternative metallacycles, via pathways 1 and 2, are shown in Schemes 10–12. While in the

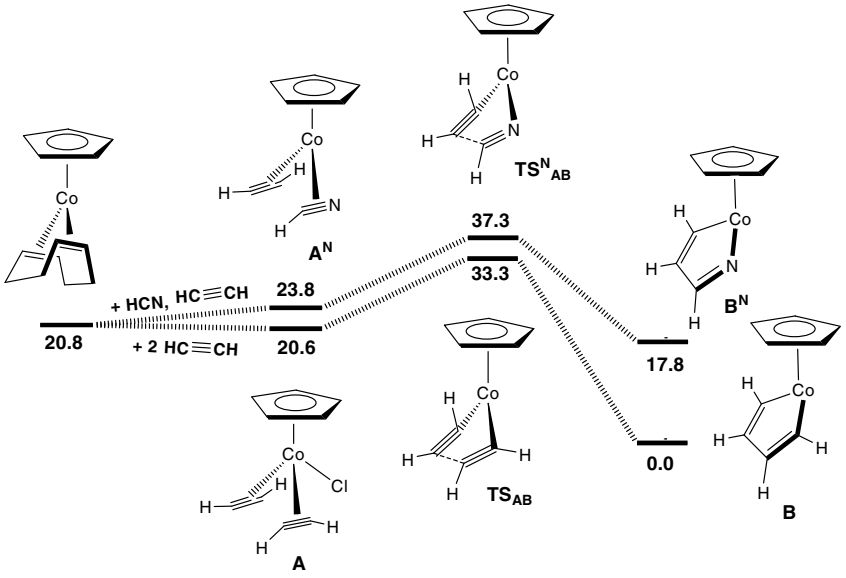

Scheme 9. Free energy profile (in kcal mol^{-1}) for the conversion of CoCp(COD) via the bis(alkyne)complexes A and A^N into the respective metallacycles B and B^N.

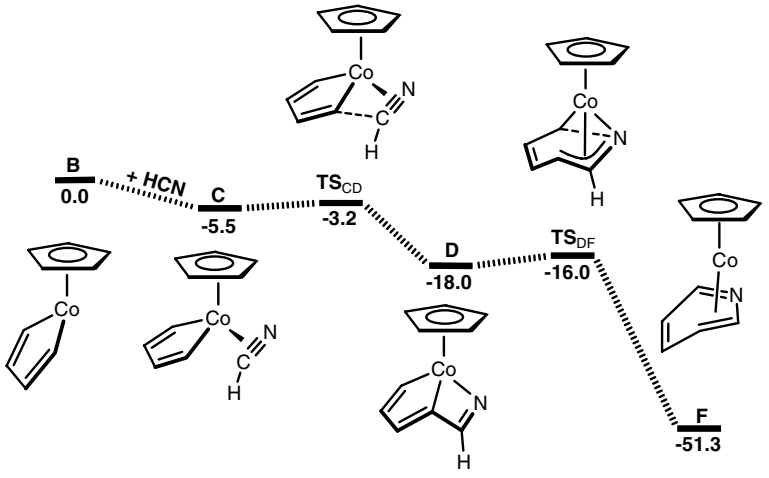

Scheme 10. Free energy profile (in kcal mol^{-1}) for the conversion of the metallacycle B into the η^4-pyridine complex F with N≡C–H.

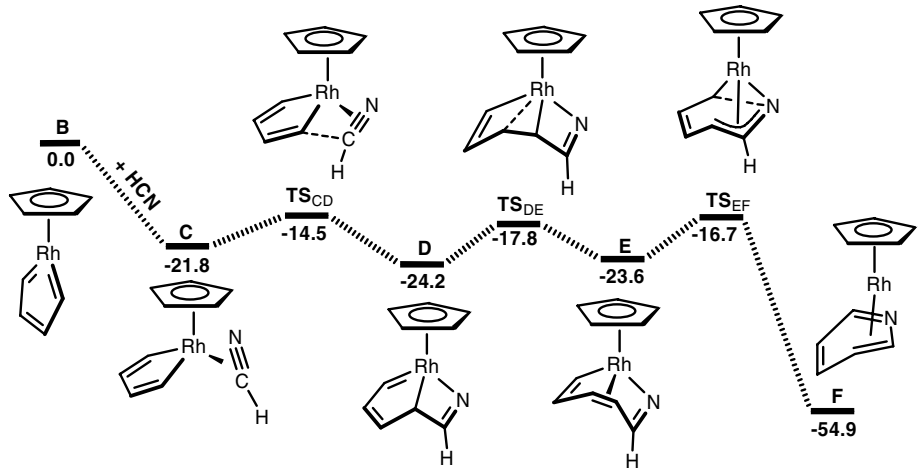

Scheme 11. Free energy profile (in kcal mol^{-1}) for the conversion of the rhodium metallacycle B into the η^4-pyridine complex F with N≡C–H.

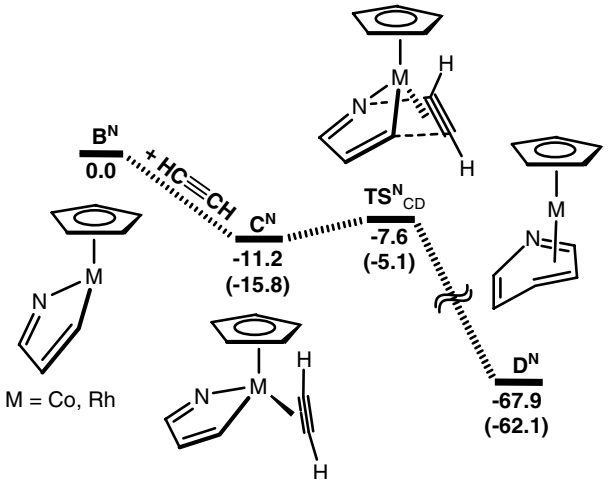

Scheme 12. Free energy profile (in kcal mol^{-1}) for the conversion of the cobalt and rhodium aza metallacycle B^N into the η^4-pyridine complex D^N (free energies for Rh are in parenthesis).

case of Co, both paths A and B involve comparable energies, in the case of Rh path A seems to be favored.

For pathway 1, the overall reaction steps are similar to those of the ones described for the RuCpCl system. The origin of the few dissimilarities between the Co and Rh system and CpRuCl can be traced partly to the absence of the Cl coligand, namely unfavorable steric interactions due to substituents at the acetylene and/or nitrile ligands are less pronounced. Another obvious difference concerns the structure of the metallacycloheptatriene E, an intermediate only detected in the RhCp system. In addition to the Rh–C bond and Rh–N single bonds, π-bonding of the internal olefinic double bond takes place (Rh–C distances of 2.31 and 2.26 Å, Fig. 6), satisfying the 18-electron rule. In the case of cobalt this intermediate could not be located and the bicylic complex D was found to rearrange directly to afford F, where the pyridine ligand is coordinated in η^4-fashion. Completion of the cycle A is achieved via the reaction F + 2HC≡CH → pyridine + A, which is exergonic by 34.8 and 26.0 kcal/mol for M = Co and Rh, respectively, showing that pyridine displacement is indeed thermodynamically accessible.

The optimized structures of intermediate D for Co and Rh, as well as intermediate E, are depicted in Fig. 6. Although intermediate D can be schematically represented in a similar way for both Co and Rh, the internal bonds are significantly different, especially the central M–C bond, is much longer for Co (2.49 Å) than for Rh (2.10 Å). Moreover, in the case of Rh, D features a Rh=C double bond (1.90 Å). The sequence of C–C and C=C bonds is also different for the two species. It is thus not very surprising that the pathway differs from this point on.

The free energy profile for pathway 2 is given in Scheme 12 for both Co and Rh. The azametallacycle B^N is able to accommodate another alkyne to afford the metallacyclopendiene acetylene complex C^N. This process is thermodynamically very favorable releasing 11.2 and 15.8 kcal/mol for M = Co and Rh, respectively. C^N undergoes a facile

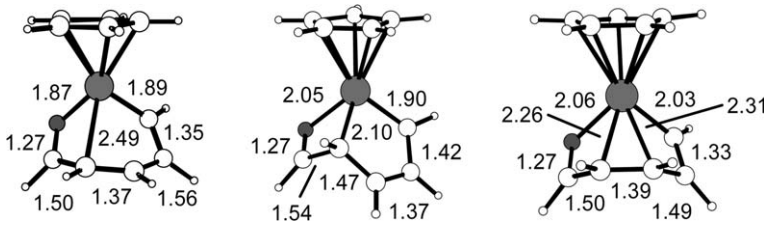

Fig. 6. Optimized geometry (distances in Å) of the intermediate D of the CpCoCl system (left) and intermediates D and E of the CpRh system.

[4+2] cycloaddition, thereby forming new C–C and C–N bonds. This process takes place in a concerted fashion (cf. C vs. N-site attack in the case of the RuCpCl system according to Schemes 6 and 7) yielding the η^4-pyridine complex D^N. This transformation is strongly exergonic with a rather small free energy barrier of 2.6 kcal/mol for M = Co and a moderate barrier of 10.0 kcal/mol for M = Rh.

3. Conclusion

In sum we have established reasonable pathways for the RuCpCl, CoCp, and RhCp catalyzed cyclocotrimerization of two alkynes and the nitriles N≡CR (R = H, Me, Cl, COOMe) to afford pyridines. According to the proposed mechanism, the key reaction step is the oxidative coupling of two alkyne ligands to give metallacyclopentatriene (Ru, Rh) and metallacyclopentadiene (Co) intermediates. In the case of ruthenium, this process is thermodynamically clearly favored over the oxidative coupling between one alkyne and one nitrile ligand to afford an elusive azametallacycle. Moreover, even if an azametallacycle is formed, the subsequent reaction with an alkyne would result in the formation of an exceptionally stable bicyclic intermediate which essentially may be regarded as a dead-end product. Consequently, this pathway may be dismissed as non competitive. This alternative pathway however cannot be dismissed in the case of Co and Rh. The rate determining step of the overall catalytic cycle is the addition of the nitrile to the five-membered metallacycles which has to take place in a side-on fashion. Competitive alkyne addition leads to benzene formation and, accordingly, also the chemoselectivity of this reaction is controlled at this stage of the catalytic cycle. In the case of the RuCpCl fragment, the addition of nitriles R–C≡N and acetylenes RC≡CH has been investigated in more detail. For R = H, Cl, and COOMe the side-on addition of nitriles is kinetically more favored than alkyne addition and, in accordance with experimental results, pyridine formation takes place. In the case of R = Me nitrile addition appears to be strongly disfavored and the addition of alkynes to give benzenes is kinetically preferred. Once the nitrile is coordinated, facile C–C bond coupling takes place to afford an unusual five- and four-membered bicyclic ring system which eventually rearranges to a very unsymmetrical azametallaheptatriene complex which in turn provides CpRuCl(κ^1-pyridine) via a reductive elimination step. Completion of the catalytic cycle is achieved by an exergonic displacement of the respective pyridine product by two acetylene molecules regenerating the bisacetylene complex.

4. Experimental

4.1. Computational techniques

All calculations were performed using the GAUSSIAN03 software package [15] on the Silicon Graphics Cray Origin 2000 of the Vienna University of Technology. The geometry and energy of the model complexes and the transition states were optimized at the B3LYP level with the Stuttgart/Dresden ECP (sdd) basis set [22] to describe the electrons of the ruthenium, cobalt, and rhodium atoms. For all other atoms the 6–31g** basis set was employed [23]. Frequency calculations were performed to confirm the nature of the stationary points, yielding one imaginary frequency for the transition states and none for the minima. Each transition state was further confirmed by following its vibrational mode downhill on both sides, and obtaining the minima presented on the reactions free energy profile. All geometries were optimized without constraints (C_1 symmetry) and the energies were zero point corrected. Relative energies were compared taking into account the total number of molecules present.

The energy decomposition analysis was carried out with the Amsterdam Density Functional program (ADF-2004) [20]. Vosko, Wilk and Nusair's local exchange correlation potential [24] was used with Perdew–Wang non-local exchange correlation corrections [25]. Relativistic effects were treated by the ZORA formalism [26]. The core orbitals were frozen for Ru ([1–3]s, [2–3]p, 3d), Cl ([1–2]s, 2p), and C, N and O (1s). Triple ζ Slater-type orbitals (STO) were used to describe the valence shells C, N, O (2s and 2p), Cl (3s, 3p), and Ru (4d, 5s). A set of two polarization functions was added to C, O (single ζ, 3d, 4f), P, S (single ζ, 3d, 4p), and Ru (single ζ, 5p, 4f). Triple ζ Slater-type orbitals (STO) were used to describe the valence shells of H (1s) with two polarization functions (single ζ, 2p, 3d).

The geometries obtained from the calculations with GAUSSIAN03 and described above (Scheme 4) were used.

Acknowledgements

Financial support by the "Fonds zur Förderung der wissenschaftlichen Forschung" (Project No. P16600-N11) is gratefully acknowledged. P.J.C. acknowledges FCT for a Grant (SFRH/BD/10535/2002). M.J.C. and P.J.C. thank FCT for financial support (project POCI/QUI/58925/2004).

Appendix A. Supplementary data

Supplementary data associated with this article can be found, in the online version, at doi:10.1016/j.jorganchem.2006.03.004.

References

[1] S. Niu, M.B. Hall, Chem. Rev. 100 (2000) 353.
[2] (a) I. Nakamura, Y. Yamamoto, Chem. Rev. 104 (2004) 2127;
(b) J.A. Varela, C. Saa, Chem. Rev. 103 (2003) 3787;
(c) U.M. Dzhemilev, F.A. Selimov, G.A. Tolstikov, ARKIVOC ix (2001) 85.
[3] (a) D. Suzuki, R. Tanaka, H. Urabe, F. Sato, J. Am. Chem. Soc. 124 (2002) 3518;
(b) K. Takai, M. Yamada, K. Utimoto, Chem. Lett. (1995) 851;

(c) J.E. Hill, G. Balaich, P.E. Fanwich, I.P. Rothwell, Organometallics 12 (1993) 2911;
(d) D.P. Smith, J.R. Strickler, S.D. Gray, M.A. Bruck, R.S. Holmes, D.E. Wigley, Organometallics 11 (1992) 1275;
(e) C. Bianchini, A. Meli, M. Peruzzini, A. Vacca, F. Vizza, Organometallics 10 (1991) 645.

[4] (a) T. Takahashi, F.-Y. Tsai, M. Kotora, J. Am. Chem. Soc. 122 (2000) 4994;
(b) T. Takahashi, F.-Y. Tsai, Y. Li, H. Wang, Y. Kondo, M. Yamanaka, K. Nakajima, M. Kotora, J. Am. Chem. Soc. 124 (2002) 5059.

[5] (a) U. Schmidt, U. Zenneck, J. Organomet. Chem. 440 (1992) 187;
(b) F. Knoch, F. Kremer, U. Schmidt, U. Zenneck, Organometallics 15 (1996) 2713.

[6] (a) Y. Yamamoto, K. Kinpara, T. Saigoku, H. Takagishi, S. Okuda, H. Nishiyama, K. Itoh, J. Am. Chem. Soc. 127 (2005) 605;
(b) Y. Yamamoto, R. Ogawa, K. Itoh, J. Am. Chem. Soc. 123 (2001) 6189;
(c) Y. Yamamoto, S. Okuda, K. Itoh, Chem. Commun. (2001) 1102;
(d) J.A. Varela, L. Castedo, C. Saa, J. Org. Chem. 68 (2003) 8595.

[7] (a) H. Bönnemann, Angew. Chem. Int. Ed. Engl. 24 (1985) 248;
(b) H. Bönnemann, W. Brijoux, Adv. Heterocycl. Chem. 48 (1990) 177.

[8] P. Diversi, L. Ermini, C. Ingrosso, A. Lucherini, J. Organomet. Chem. 447 (1993) 291.

[9] M.M. McCormick, H.A. Duong, G. Zuo, J. Louie, J. Am. Chem. Soc. 127 (2005) 5030.

[10] K. Kirchner, M.J. Calhorda, R. Schmid, L.F. Veiros, J. Am. Chem. Soc. 125 (2003) 11721.

[11] Y. Yamamoto, T. Arakawa, R. Ogawa, K. Itoh, J. Am. Chem. Soc. 125 (2003) 12143.

[12] (a) J.H. Hardesty, J.B. Koerner, T.A. Albright, G.Y. Lee, J. Am. Chem. Soc. 121 (1999) 6055;
(b) Y. Wakatsuki, O. Nomura, K. Kitaura, K. Morokuma, H. Yamazaki, J. Am. Chem. Soc. 105 (1983) 1907;
(c) A.A. Dehy, N. Koga, Bull. Chem. Soc. 78 (2005) 781;
(d) A.A. Dehy, C.H. Suresh, N. Koga, Bull. Chem. Soc. 78 (2005) 792.

[13] (a) M.J. Calhorda, K. Kirchner, L.F. Veiros, in: C.G. Screttas, B.R. Steele (Eds.), Perspectives in Organometallic Chemistry, The Royal Society of Chemistry, Cambridge, 2003, pp. 111–119;
(b) E. Rüba, R. Schmid, K. Kirchner, M.J. Calhorda, J. Organomet. Chem. 682 (2003) 204;
(c) R. Schmid, K. Kirchner, J. Org. Chem. 68 (2003) 8339;
(d) G. Dazinger, R. Schmid, K. Kirchner, New J. Chem. (2004) 153;
(e) L.F. Veiros, G. Dazinger, K. Kirchner, M.J. Calhorda, R. Schmid, Chem. Eur. J. 10 (2004) 5860.

[14] (a) A.D. Becke, J. Chem. Phys. 98 (1993) 5648;
(b) B. Miehlich, A. Savin, H. Stoll, H. Preuss, Chem. Phys. Lett. 157 (1989) 200;
(c) C. Lee, W. Yang, G. Parr, Phys. Rev. B 37 (1988) 785.

[15] M.J. Frisch, G.W. Trucks, H.B. Schlegel, G.E. Scuseria, M.A. Robb, J.R. Cheeseman, J.A. Montgomery Jr., T. Vreven, K.N. Kudin, J.C. Burant, J.M. Millam, S.S. Iyengar, J. Tomasi, V. Barone, B. Mennucci, M. Cossi, G. Scalmani, N. Rega, G.A. Petersson, H. Nakatsuji, M. Hada, M. Ehara, K. Toyota, R. Fukuda, J. Hasegawa, M. Ishida, T. Nakajima, Y. Honda, O. Kitao, H. Nakai, M. Klene, X. Li, J.E. Knox, H.P. Hratchian, J.B. Cross, C. Adamo, J. Jaramillo, R. Gomperts, R.E. Stratmann, O. Yazyev, A.J. Austin, R. Cammi, C. Pomelli, J.W. Ochterski, P.Y. Ayala, K. Morokuma, G.A. Voth, P. Salvador, J.J. Dannenberg, V.G. Zakrzewski, S. Dapprich, A.D. Daniels, M.C. Strain, O. Farkas, D.K. Malick, A.D. Rabuck, K. Raghavachari, J.B. Foresman, J.V. Ortiz, Q. Cui, A.G. Baboul, S. Clifford, J. Cioslowski, B.B. Stefanov, G. Liu, A. Liashenko, P. Piskorz, I. Komaromi, R.L. Martin, D.J. Fox, T. Keith, M.A. Al-Laham, C.Y. Peng, A. Nanayakkara, M. Challacombe, P.M.W. Gill, B. Johnson, W. Chen, M.W. Wong, C. Gonzalez, J.A. Pople, GAUSSIAN 03, Gaussian, Inc., Pittsburgh, PA, 2003.

[16] For calculations of end-on vs side-on coordinated nitriles see: C.-F. Huo, T. Zeng, Y.-W. Li, M. Beller, H. Jiao, Organometallics 24 (2005) 6037.

[17] S. Portmann, H.P. Lüthi, Chimia 54 (2000) 766.

[18] M.J. Calhorda, M.A.A.F. de C. T. Carrondo, A.R. Dias, A.M.T. Domingos, M.T.L.S. Duarte, M.H. Garcia, C.C. Romão, J. Organomet. Chem. 320 (1987) 63.

[19] H. Wadepohl, U. Arnold, H. Pritzkov, M.J. Calhorda, L.F. Veiros, J. Organomet. Chem. 587 (1999) 233.

[20] (a) G. te Velde, F.M. Bickelhaupt, S.J.A. van Gisbergen, C.F. Guerra, E.J. Baerends, J.G. Snijders, T. Ziegler, J. Comput. Chem. 22 (2001) 931;
(b) C.F. Guerra, J.G. Snijders, G. te Velde, E.J. Baerends, Theor. Chem. Acc. 99 (1998) 391;
(c) ADF2005.01, SCM, Theoretical Chemistry, Vrije Universiteit, Amsterdam, The Netherlands..

[21] (a) T. Ziegler, A. Rauk, Inorg. Chem. 18 (1979) 1755;
(b) T. Ziegler, A. Rauk, Theor. Chim. Acta 46 (1977) 1.

[22] (a) U. Haeusermann, M. Dolg, H. Stoll, H. Preuss, Mol. Phys. 78 (1993) 1211;
(b) W. Kuechle, M. Dolg, H. Stoll, H. Preuss, J. Chem. Phys. 100 (1994) 7535;
(c) T. Leininger, A. Nicklass, H. Stoll, M. Dolg, P. Schwerdtfeger, J. Chem. Phys. 105 (1996) 1052.

[23] (a) A.D. McClean, G.S. Chandler, J. Chem. Phys. 72 (1980) 5639;
(b) R. Krishnan, J.S. Binkley, R. Seeger, J.A. Pople, J. Chem. Phys. 72 (1980) 650;
(c) A.H. Wachters, Chem. Phys. 52 (1970) 1033;
(d) P.J. Hay, J. Chem. Phys. 66 (1977) 4377;
(e) K. Raghavachari, G.W. Trucks, J. Chem. Phys. 91 (1989) 1062;
(f) R.C. Binning, L.A. Curtiss, J. Comput. Chem. 103 (1995) 6104;
(g) M.P. McGrath, L. Radom, J. Chem. Phys. 94 (1991) 511.

[24] S.H. Vosko, L. Wilk, M. Nusair, Can. J. Phys. 58 (1980) 1200.

[25] J.P. Perdew, J.A. Chevary, S.H. Vosko, K.A. Jackson, M.R. Pederson, D.J. Singh, C. Fiolhais, Phys. Rev. B46 (1992) 6671.

[26] E. van Lenthe, A. Ehlers, E.J. Baerends, J. Chem. Phys. 110 (1999) 8943.